Analysis of thundercloud electrostatic field during a lightning strike to a FALCON 20

Magalie Buguet, Pierre Laroche, Philippe Lalande, Aurélie Bouchard, Patrice Blanchet, Arnaud Chazottes

ANALYSIS OF THUNDERCLOUD ELECTROSTATIC FIELD DURING A LIGHTNING STRIKE TO A FALCON 20

Magalie Buguet, Pierre Laroche, **Philippe Lalande**, Aurélie Bouchard, Patrice Blanchet, Arnaud Chazottes
DPHY, ONERA, Université Paris Saclay, F-91123 Palaiseau
Palaiseau, France
lalande@onera.fr

ABSTRACT

Since the 70's, ONERA has been involved in the understanding and characterization of the physical processes occurring during a lightning strike to the aircraft which has led to the development of on board sensors for atmospheric characterization. In the 80's, a first electric field mill network had been designed to measure the electrostatic field inside thundercloud. The system was installed on a CONVAIR (CV580) and a TRANSALL (C160). A new version of this electric field mill network, called AMPERA (Atmospheric Measurement of Potential and ElectRic field on Aircraft), has been developed since 2010. From September to October 2018, an in-flight campaign was performed over Corsica (France) in the framework of EXAEDRE (EXploiting new Atmospheric Electricity Data for Research and the Environment) project to investigate the electrical activity in thunderstorm.

During this campaign, 8 scientific flights were done with a FALCON 20 (F20) of SAFIRE inside or in the vicinity of thunderstorm. During the flight of the 8 of October 2018, the aircraft was struck by lightning at an altitude of 8500m. The electrostatic field time variations show that a vertical electric polarization of the aircraft occurred just before the lightning strike. The inverse method to compute the components of the atmospheric electric field from the data of the electric field network is presented. The atmospheric electric field time evolution is shown. The value of the atmospheric electric field just before the lightning strike is about 90kV/m. This electric field value has been processed to be compared with the ones measured during TRANSALL campaigns. The altitude effect is taken into account by computing the reduced electric field (Electric field divided by air density). The comparison is presented taking into account the size of the aircraft and the electric field direction. To conclude a discussion is done on the electric field threshold for a lightning strike to aircraft.

INTRODUCTION

In the 80's, in flight campaigns have been performed to understand the physical processes occurring during a lightning strike to the aircraft when it flies in area where the atmospheric electric field generated by the thundercloud is high. This field was measured by an electric field mill network on the skin of the aircraft and its value just before a lightning strike to the aircraft was recorded. During the C160 campaign performed in the 80's (**Ref 1**, **Ref 2**), 6 values of the atmospheric field were recorded and are associated with a triggered lightning.

A new version of this electric field mill network, called AMPERA (Atmospheric Measurement of Potential and ElectRic field on Aircraft), has been developed by ONERA since 2010. In September 2018, an in-flight campaign was performed over Corsica (France) in the framework of EXAEDRE (EXploiting new Atmospheric Electricity Data for Research and the Environment) project to investigate the electrical activity in thunderstorm. During this campaign, 8 scientific flights were done with a FALCON 20 (F20) of SAFIRE (the French facility for airborne research) inside or in the vicinity of thunderstorm. During the flight of the 8 of October 2018, the aircraft was struck by lightning at an altitude of 8500m.

The purpose of this paper is to present the AMPERA system, the atmospheric field recorded during the flight leading to a lightning strike of the F20 and to present and discuss a method to compare the values measured by C160 and F20.

AMPERA

Electric Field Mill network on F20

Since the 1940s, there have been many studies estimating the atmospheric electrostatic field in fair weather conditions, but also in the vicinity and inside thunderstorms. In this framework, different kinds of airborne sensors have been developed. Design of these sensors depends on the airborne platforms that carry the instruments (Ref 3). These include, for example, the electric field meter (Ref 4, Ref 5), the rocket borne field meter, the airborne rotating vane field mill (Ref 6), the cylindrical field mill (Ref 7, Ref 3) and the rotating field mill on balloons (Ref 8, Ref 9, Ref 10). In contrast to the rocket or the balloon, the use of aircraft allows a more comprehensive temporal and spatial analysis of the electrostatic field. Aircraft

platforms have provided the only way to measure the horizontal cross-section of a cloud to date (Ref 11). From this perspective, airborne field mills have been adopted for atmospheric research by ONERA for decades (Ref 12) and tested on different kinds of aircraft (e.g. C160 Transall, Ref 1; Gloster Meteor NF11, Ref 13; Falcon 20, nowadays).
The Table 1 shows the performance and characteristics of the field mills of the AMPERA system.

Physical	Mass	0.870 kg
	Power	28V (DC) ; 25 W max
	Size	120 mm x 115 mm
Dynamic range		+/- 5 V/m to +/- 1 MV/m
Sensitivity	Below 5 kV/m	5 V/m
	Above 5kV/m	20 V/m
Sampling rate		10 Hz

Table 1 : Performance and characteristics of field mill of the AMPERA system

The integration of the 8 field mills on the F20 was done by the SAFIRE team (Table 2). Two field mills were installed on the first two windows of the cabin. Fourth were integrated to the back of pods. The two last ones are installed on ventral traps of the fuselage, one at the front one at the rear (Figure 1).

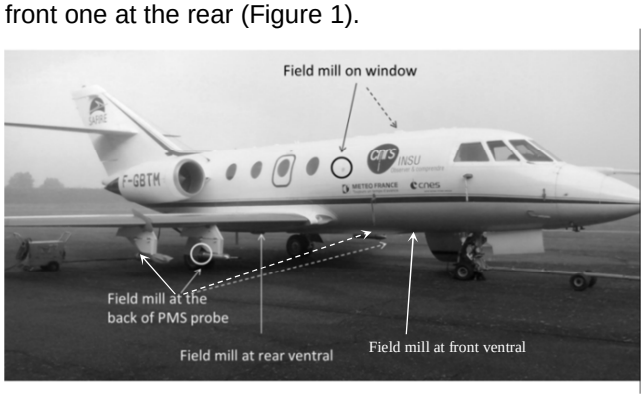

Figure 1 : Photography of the Falcon 20 (F20) of SAFIRE (http://www.safire.fr) on which the location of the 8 field mills is shown.

Name	Aircraft location
P1	Back of the external left pod
P2	Back of the internal left pod
RW	Right window (1st right window)
LW	Left window (1st left window)
P5	Back of the internal right pod
P6	Back of the external right pod
FV	Front ventral
RV	Rear ventral

Table 2 : Name and location of the field mills installed on the F20.

Inverse method

Based on the assumption of an uniform atmospheric electrostatic field around the aircraft (Ref 12, Ref 6, Ref 15, Ref 17, Ref 18, Ref 16), the electric field on the aircraft skin can be expressed by the following linear relationship:

$$E_i = \alpha_i E_x + \beta_i E_y + \gamma_i E_z + \lambda_i V_a \quad (1)$$

where Ei is the electrostatic field recorded by an individual field mill; Ex, Ey, Ez are the three components of the atmospheric electrostatic field in the aircraft reference; V is the aircraft potential; it is associated with the net electrical charge on the aircraft. The electrical charge and the potential are linked by the capacitance of the aircraft; αi, βi, λi, γi are constant coefficients. Note that these coefficients can be positive or negative except the λi coefficients which have all the same sign. This is shown by the Figure 2 which plots the electric field measured on the aircraft skin when there is only potential. The figure shows that the electric field variations are similar (in the same direction and with a same feature) from one field mill to an other.

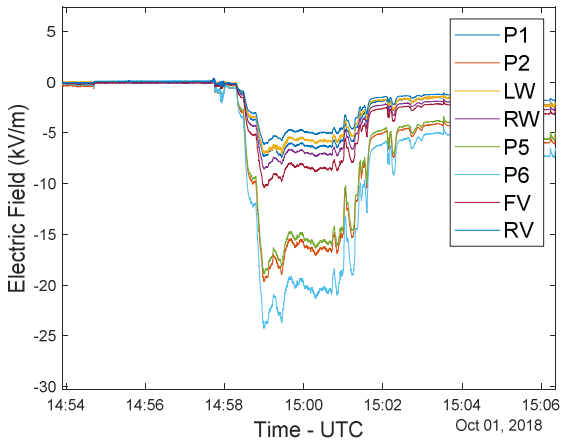

Figure 2: Electric field on the electric field mill on the F20 the 1st of October 2018.

The atmospheric electric field components and the electric potential of the aircraft are computed from:

$$\begin{bmatrix} E_x \\ E_y \\ E_z \\ V_a \end{bmatrix} = A^T (A.A^T)^{-1} \begin{bmatrix} E_1 \\ \vdots \\ E_8 \end{bmatrix} \quad (2)$$

Where $A = \begin{pmatrix} \alpha_1 & \cdots & \lambda_1 \\ \vdots & \ddots & \vdots \\ \alpha_8 & \cdots & \lambda_8 \end{pmatrix}$

In the EXAEDRE campaign, these coefficients have been derived in two steps. In a first step, a Poisson equation solver has been used to numerically compute the value of Ei based on the three-dimensional shape model (Figure 3) of the Falcon 20 aircraft. In a second step, the computed coefficients have been tuned from in-flight calibration in fair weather (Ref 18, Ref 14, Ref 5).

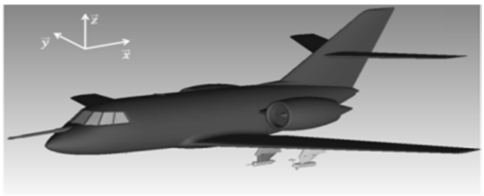

Figure 3 : Three dimensional shape model of the Falcon 20 aircraft including the pods.

FLIGHT OF THE 8 OF OCTOBER 2018

The aircraft took off at 7h30 UTC from Solenzara in Corsica and landed after 11h00 UTC.

Weather condition

The flight route was at the west of Corsica above the Mediterranean sea and at the north frontier of a huge convective zone which was developing (Figure 4) from the south to the north. The maximum altitude of cloud top was 11 000m (red color).

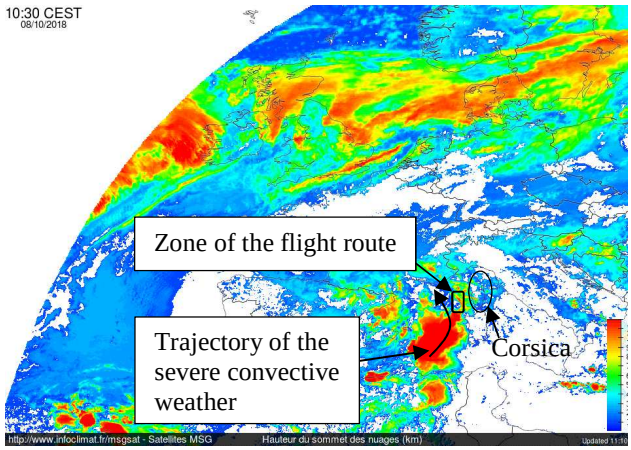

Figure 4: Image of altitude of cloud top (www.infoclimat.fr, MSG satellite) at 10h30UTC. The red color is associated with an altitude of 11 000m.

The Blitzortung lightning detection network showed at 10h30 UTC an intense lightning activity with 1000 flashes in the last 20 minutes (Figure 5) developing from the south to the north.

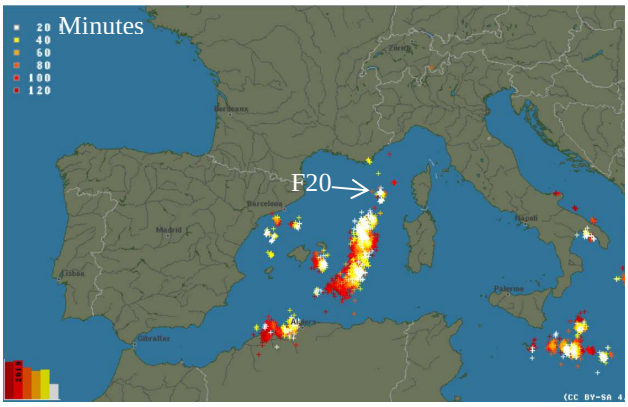

Figure 5: Lightning activity measured by Blitzortung lightning detection network at 10h30 UTC (www.blitzortung.org). The flash location is shown by a cross which color is associated with the datation of the flash. The color scale is split with a time interval of 20 minutes.

Flight route

The aircraft flew inside and near isolated convective by describing some loops (Figure 6). During the flight and the measurement, the altitude of the aircraft was from 6 000m to 10 000m (Figure 7).

At 10h40'59", the aircraft is struck by lightning and the crew has to stop the flight. The Figure 9 shows a photo of the lightning flash attached on the boom of the F20. The picture was taken from the cockpit.

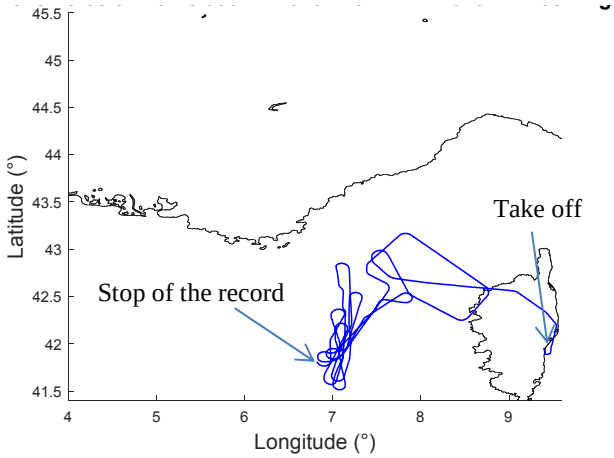

Figure 6: Route of the flight the 8 of October 2018. The route from 10h44UTC to the landing is not shown.

The Figure 8 shows the flight route of the aircraft during the last 20 minutes before the lightning strike superimposed to the radar echoes of precipitation (Figure 8). The altitude is from 7500m to 8500m. The lightning occurred when the aircraft (black filled circle) is at 8500m near an intense precipitation zone.

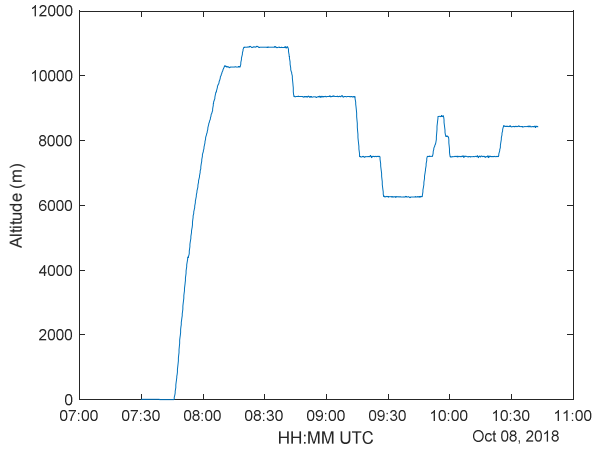

Figure 7: Altitude of the aircraft during the flight.

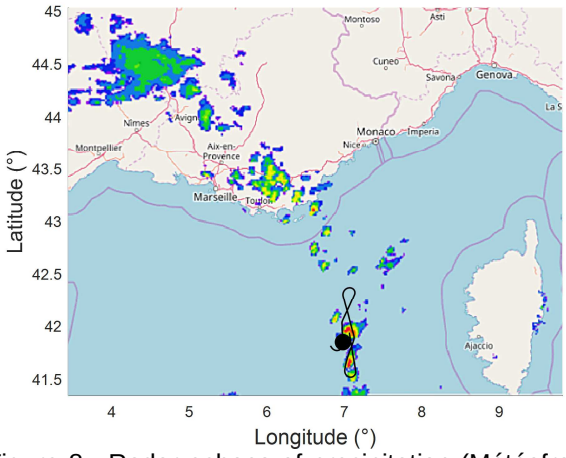

Figure 8 : Radar echoes of precipitation (Météofrance) at 10h30UTC 08/10/2018 on which are superimposed the location of the lightning strike (black-filled circle) and the route of the flight (black line). The route flight shown is between 10h20 and 10h44UTC.

Figure 9 : Photography of the lightning strike to the Falcon 20. The lightning is attached on the front boom. The photography is taken from the cockpit window.

ATMOSPHERIC ELECTRIC FIELD MEASUREMENTS

The Figure 10 shows the time variation of the electric field measured by each electric field mill for the last 20 minutes before the lightning strike. The field mill measured electric field from -300 kV/m to 100 kV/m. The duration can be split in 5 main sequences associated with a penetration of the aircraft inside the cloud (Figure 10, Figure 11). The period during which the electric field is low on the field mill corresponds to flight route mainly outside or near the cloud (Figure 11) except for the second point.

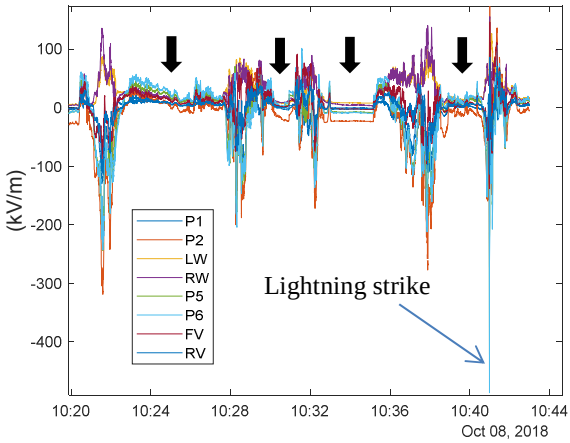

Figure 10 : Time evolution of the electric field measured by each field mill the 8 of October 2018. The time is UTC. The black arrows show the time of the aircraft when it arrives to a square of Figure 11.

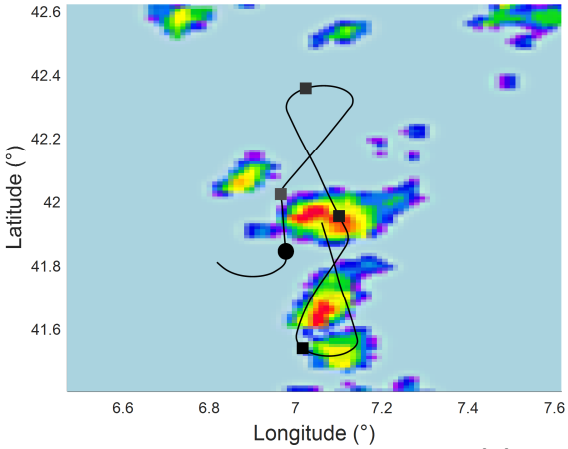

Figure 11 : Radar echoes of precipitation (Météofrance) at 10h30UTC 08/10/2018 on which are superimposed the location of the lightning strike (black-filled circle) and the route of the flight (black line). The route flight shown is between 10h20 and 10h44UTC. The square indicates the location of the aircraft for the time shown by the black arrow of Figure 10.

In the Figure 12, 2 minutes around the lightning strike is plotted. At 10h40'30" the measurements show that there is a vertical polarization of the aircraft. The electric field measured by the field mills on the fuselage windows (LW, RW) increases and is positive while on the other field mills it decreases and is negative.

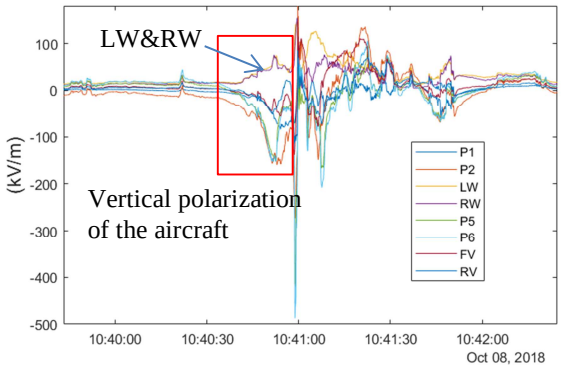

Figure 12 : Electrostatic fields measured by the 8 field mills on the fuselage around the lightning strike time.

For the other sequence, it is more complex to directly analyze the signal coming from the field mills without using the inverse method to retrieve the atmospheric electric field component and the aircraft potential. The method describes by the equation 2 has been applied to these 5 sequences. The Figure 13 shows that the main component of the atmospheric electric field is vertical with a maximum of 87kV/m. The aircraft potential reaches a maximum of 350 kV associated with a negative net electric charge. It decreases few seconds later to 160 kV just before the lightning strike.

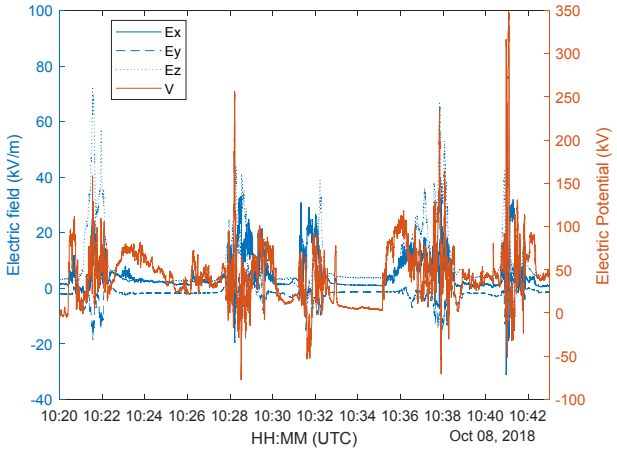

Figure 13 : Time evolution of the atmospheric electrostatic field components (Ex,Ey,Ez) in the aircraft reference and the electrical potential of the aircraft.

The Figure 14 shows the module of the atmospheric electric field during these last 20 minutes. The electric field leading to the lightning strike is of 90 kV/m.

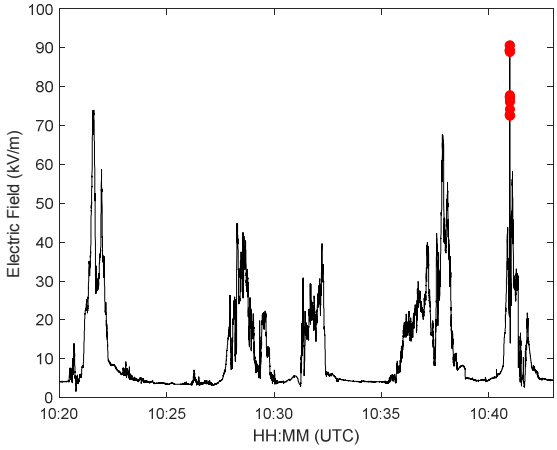

Figure 14 : Time evolution of the module of the atmospheric electrostatic field. The red filled circles are associated with the electrostatic field variation during the lightning strike.

ANALYSIS AND DICUSSIONS

The Table 3 and Table 4 show the value of the atmospheric electric field just before a lightning strike for the F20 and the C160. The sign of the electric potential for the F20 is changed to respect the convention used for the C160. The electric potential is negative when a negative net electric charge is on the aircraft.

N°	Ex (kV/m)	Ey (kV/m)	Ez (kV/m)	E (kV/m)	V (kV)	Alt (km)
1	33	-19	-40	55	-1950	4.6
2	45	-7	-26	52	-840	4.2
3	31	15	-60	69	85	4.2
4	-30	14	-29	44	-157	4.2
5	58	-5	17	61	-1335	4.2
6	37	-36	-54	75	-1890	4.2

Table 3 : Atmospheric electrostatic field measured on C160 just before the lightning strike to the aircraft.

N°	Ex (kV/m)	Ey (kV/m)	Ez (kV/m)	E (kV/m)	V (kV)	Alt (km)
1	10	20	87	90	-160	8.5

Table 4 : Atmospheric electrostatic field measured on F20 just before the lightning strike to the aircraft.

A direct comparison is not obvious because the size of these aircrafts is quite different. The C160 is about twice longer than a F20. Moreover, the altitude of the lightning are also different.
In Ref 19, Lalande et al. have shown that lightning leader inception depends on the air density and on the electric length of the objet from which the lighting develops (Ref 20).
In order to take into account these dependencies, the atmospheric electric field measured by the F20 has been postprocessing as follow:

- The effect of altitude is taking into account by dividing the atmospheric electric field value by the air density at the flight level. The density is given by the following expression

$$\delta = \frac{P}{P_o}.\frac{T_o}{T} \quad (3)$$

Where Po and To are the pressure and temperature at mean sea level. P and T are the pressure and temperature at the flight level. P and T can be expressed as a function of the altitude z (km) by using:

$$\frac{P}{P_o} = \exp\left(-\frac{z}{8}\right) \quad (4)$$

$$T = T_o - 6.z \quad \text{with To is set to 293K.} \quad (5)$$

- The electric length of the aircraft depends on the direction of the atmospheric electric field in regard with the aircraft orientation. If the electric field component is vertical, the length is the height of the aircraft. If the field is along the fuselage, the electric length is the aircraft length. For a given atmospheric electric field direction, the electric length H of the aircraft is computed as follow:
  - The geometry of the aircraft is projected on a line generated by the field direction $\vec{E}$ (Figure 15)
  - The electric length of the aircraft for this electric field direction is the distance H (Figure 15).

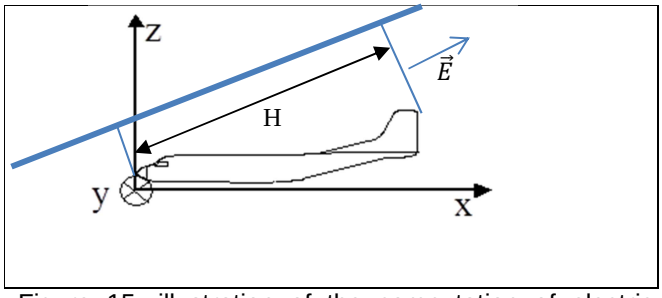

Figure 15: illustration of the computation of electric length H of the aircraft for a given direction of the atmospheric electric field $\vec{E}$.

The result of this processing is shown in the Figure 16. The module of the atmospheric electric field brought back to the mean sea level (reduced electric field) is plotted as a function of the electric length of the aircraft. The black dots are associated with the F20 flight of the 8 of October 2018. The red filled circles are associated with the lightning strike (Figure 14). The black diamonds correspond to the lightning strikes of the C160.
The figure shows that the effect of the electric length on the lightning triggered threshold. The longer the aircraft is, the lower the electric field to trigger a lightning is. The analytical expression of equation 6 has been plotted on the figure (E_{stab}). It delimits a border between a zone of high probability of lightning strike to a zone of low probability.

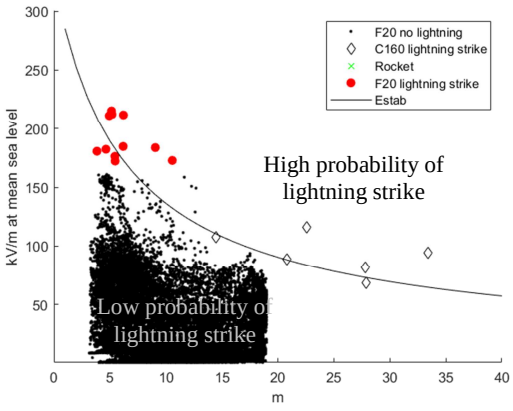

.

Figure 16 : Comparison between atmospheric electrostatic field threshold for F20 and C160 as a function of the electrical length of the aircraft (H).

$$E_{Stab}(H) = \left[\frac{306.7}{1+\frac{H}{6.1}} + \frac{21.6}{1+\frac{H}{134.7}}\right].\delta \quad (6)$$

This simple analytical expression fits quite well the data. It takes into account the altitude and the aircraft geometry. It could be a valuable expression, derived from experiment, to be used in zoning computation.

However, this method needs further validations by measuring the atmospheric electric threshold to trigger a lightning strike on other size of aircraft and other altitudes.

CONCLUSION

During the EXAEDRE in flight campaign, ONERA has measured the atmospheric electric field by using the AMPERA system. It is composed of a set of 8 field mill sensors.

The 8 of October 2018, the F20 of SAFIRE was flying in the frontier of a huge convective zone developing from the south to the north at the west of Corsica above the sea.

At 10h40'59", the aircraft was struck by lightning at an altitude of 8500m. The atmospheric electric field just before the lightning strike is 90 kV/m and the aircraft electric potential is -350 kV.

In order to compare, this value to the ones obtained during C160 in flight campaign, a method was proposed to take into account the altitude effect and the size of the aircraft. An analytical expression given the electric field threshold to trigger a lightning from an aircraft is given. It only depends of the air density and the electric length of the aircraft. It is a preliminary method which has to be tested with some others results.

AKNOWLEDGEMENT

The EXAEDRE project is sponsored by grant ANR-16-CE04-0005 with support from CNES and MISTRALS/HyMeX.

REFERENCES

Ref 1: Delannoy A., Gondot P, 2012: Airborne Measurements of the Charge of Precipitating Particles Related to Radar Reflectivity and Temperature within two Different Convective Clouds, Journal of Aerospace Lab, AL05-02.

Ref 2: Laroche P., Delannoy A., Issac F., 2012 Experimental Studies of Lightning Strikes to Aircraft, Journal of Aerospace Lab,, AL05-06.

Ref 3: MacGorman D. and Rust W. D., 1998: The electrical nature of storms, Oxford University Press, 422p.

Ref 4: Gun R. 1948: Electric Field Intensity Inside of Natural Clouds, *J. Applied Physics*, **19**, 481-484.

Ref 5: Winn W. P., 1993: Aircraft Measurement of Electric Field: Self-Calibration, *J. Geophysical Res*., **98**, 7351-7365.

Ref 6: Jones, J. J., 1990: Electric Charge Acquired by Airplanes Penetrating Thunderstorms, *J. of Geo. Res*., **95**, No, D10, 16589-16600.

Ref 7: Kasemir H. W. 1972: The cylindrical field mill, *Meteor. Rundshau*, **25**, 33-38.

Ref 8: Chauzy S., Médale J.-C., Prieur S., Soula S., 1991 : Multilevel measurement of the electric field underneath a thundercloud. 1. A new system and the associated data processing. J. G. R., 96, 22319-22326.

Ref 9: Marshall T., Rust W. D., 1991: Electric Field Soundings Through Thunderstorms, J. G. R., **96**, 22297-22306.

Ref 10: Stolzenburg M., Rust W. D., Smull B. F., Marshall T. C., 1998: Electrical structure in thunderstorm convective regions. 1. Mesoscale convective systems, J. G. R., 103, 14059-14079.

Ref 11: Christian Jr. H. J., 1976: Design and evaluation of balloon-borne electric field sensor, *Rice University, Thesis*, 78p.

Ref 12: Laroche P. 1986: Airborne measurements of electrical atmospheric field produced by convective clouds, *Rev. Phys. App.*, 809-815.

Ref 13: Boulay J. L., Laroche P., 1982: Aircraft Potential Variations In flight, Int. *Aerospace Conference on Lightning and Static Electricity*, 19.

Ref 14: Bateman M. G., Stewart M. F., Blakeslee R. J., Podgorny S. J., Christian H. J., Mach D. M., Bailey J. C., Daskar D., 2007: A low noise, Microprocessor-Controlled, Internally Digitizing Roating-Vane Electric Field Mill for Airborne Platforms. *J. Atmos. and Ocea. Tech.*, **24**, 1245-1255.

Ref 15: Mach D.M. and Koshak W. J., 2007: General Matrix Inversion Technique for the Calibration of Electric Field Sensor Arrays on Aircraft Platforms, *J. Atmos. Oceanic Tech*, **24**, 1576 – 1587.

Ref 16: Mach D. M. 2015: Technique for Reducting the Effects of Nonlinear Terms on Electric Field Measurements of Electric Field Sensor Arrays on Aircraft Platforms, J. Atmos. Oceanic Tech, **32**, 993-1003.

Ref 17: Koshak W. J., Bailey J., Christian H. J., Mach D. M., 1994: Aircraft electric field measurements: Calibration and ambient field retrieval, *J. Geo. Res*., **99**, D11, 2281 – 22792.

Ref 18: Koshak W. J., 2006: Retrieving Storm Electric Fields from Aircraft Field Mill Data. Part I: Theory, L. Atmos. Ocea. Tech, 23, 1289-1302.

Ref 19: P. LALANDE, A. BONDIOU-CLERGERIE, G. BACCHIEGA, I. GALLIMBERTI – 2002 Observations and Modeling of Lightning Leaders.

Comptes Rendus Physique, vol. 3, no. 10, p. 1375-1392,.
Ref 20: WILLETT, D. . DAVIS, P. LAROCHE – 1999 An Experimental Study of Positive Leaders Initiating Rocket-Triggered Lightning. Atmospheric Research, vol. 51, no. 3-4, p. 189-219, juill.